Aalborg Universitet

AALBORG UNIVERSITY
DENMARK

Double Layered Sheath in Accurate HV XLPE Cable Modeling

Gudmundsdottir, Unnur Stella; Silva, J. De; Bak, Claus Leth; Wiechowski, W.

Published in:
Proceedings of the PES General Meeting 2010

DOI (link to publication from Publisher):
10.1109/PES.2010.5589893

Publication date:
2010

Document Version
Accepted author manuscript, peer reviewed version

Double Layered Sheath in Accurate HV XLPE Cable Modeling

U. S. Gudmundsdottir, *Student Member, IEEE,* J. De Silva, *Member, IEEE*, C. L. Bak, *Senior Member IEEE*, and W. Wiechowski, *Senior Member IEEE*

Abstract-- **This paper discusses modelling of high voltage AC underground cables. For long cables, when crossbonding points are present, not only the coaxial mode of propagation is excited during transient phenomena, but also the intersheath mode. This causes inaccurate simulation results for high frequency studies of crossbonded cables. For the intersheath mode, the correct physical representation of the cables sheath as well as proximity affect play a large role and will ensure correct calculations of the series impedance matrix and therefore a correct simulation for the actual cable. This paper gives a new, more correct method for modelling the actual physical layout of the sheath. It is shown by comparison to field measurements how the new method of simulating the cable's sheath results in simulations with less deviation from field test results.**

***Index Terms*-- Insulated cables, modeling, power system transients, simulation, model accuracy, XLPE cables, wave propagation, modal excitation.**

I. Introduction

NOWADAYS, extruded (XLPE) cables are the most common cable types in HV underground cable systems. The XLPE cable type has the advantage of having no need for auxiliary equipment and no risk of leakage as the insulation is homogeneous and without any type of fluids.

Modelling HV cables has been the topic of many previous papers [1], [2], [3], [4], [5], [6] as the modelling procedure is under constant development. The authors of this paper have previously shown [7], [8] how insufficient representation of the cables metallic sheath in the modelling software, plays a role in inaccurate simulation results for high frequency studies. This is particularly a problem for long cables where crossbonding points will cause an intersheath current wave to flow in the cable system. An analysis of a deviation between field measurements and simulation results revealed how the sheath conductor should be more accurately represented in the simulation software. The analysis revealed how the characteristics of the sheaths physical layout in the HV cable and the proximity effect should be included in the series impedance calculations.

This paper describes the properties of an XLPE cable and addresses how the physical layout of the HV underground XLPE cable can be modelled in detail in order to have a more precise simulation result. Furthermore the improved modelling procedure is verified against field measurements, where the intersheath mode is explicitly excited.

This work was supported in part the Danish Transmission operator, Energinet.dk

U. S. Gudmundsdottir is a PhD student at the Institute of Energy Technology, Aalborg University, 9220 Aalborg, Denmark (e-mail: usg@iet.aau.dk).

J. De Silva is with Manitoba HVDC Research Centre, R3J 3W1 Winnipeg, Canada (e-mail: Jeewantha@hvdc.ca)

C. L. Bak is with the Institute of Energy Technology, Aalborg University, 9220 Aalborg, Demark (e-mail: clb@iet.aau.dk).

W. Wiechowski is with Energinet.dk, 7000 Fredericisa, Denmark (e-mail: WWI@energinet.dk).

II. Layout properties of an XLPE HV cable

A layout for a typical HV single core XLPE cable is shown in Fig. 1.

Fig. 1 A typical layout for a HV XLPE cable

For the cable in Fig. 1, the cable layers are:

- Core conductor
- Semi conductive (SC) screen
- Inner insulation
- SC screen
- SC swelling tape
- Cu wires (part of sheath)
- SC swelling tape (part of sheath)
- Al laminate (part of sheath)
- Outer insulation

A. Core conductor

The purpose of the core conductor is to transmit the required current with low losses. The conductor in HV cables is either made of copper (Cu) or aluminium (Al) where Cu has a lower specific resistance. The advantage of Al over Cu, is that Al has lower mass density which leads to much less weight for the same cable capacity. For HV cables, the conductor is often stranded in order to lower the effective resistance caused by skin and proximity effect. When modelling such a non-solid conductor, the resistivity is increased according to [7], [9].

B. Inner insulation and SC screens

The purpose of the insulation is to ensure no electrical connection between the two current carrying components of the cable, the conductor and the sheath.

The SC screens are placed between the insulation and the conductor and again between insulation and the sheath. The purpose of the SC screens is to reduce the electrical stress in the inner insulation and prevent formation of voids between either core conductor or sheath and insulation due to bending of the cable or other mechanical stress.

For accurate modelling of the insulation and SC screens, the permittivity and thickness of the insulation should be corrected according to the theory [9].

C. Cable sheath

The purpose of the cable sheath is to have a metallic covering used as an electrostatic screening as well as a return path for the cable's charging current and a conduction path for earth fault current in the case of a fault on the cable.

As shown in Fig. 1, for XLPE cables, the sheath consists of several layers. The two conducting sheath layers, the wired sheath layer and the laminate layer, are separated by a SC layer and are directly connected together both at each junction and cable ends.

The laminate layer is included for water resistance. The swelling tape between the wired sheath layer and the laminate layer is SC in order to ensure no potential difference between the two conducting sheath layers in the occurrence of a failure on the cable. The two conducting layers are not touching each other in order to protect the laminate from mechanical stress because of bending and for thermal protection as the laminate can not tolerate more than 180°C while the wired sheath layer can be up to 250°C.

It is a common practise when modelling the sheath in EMT-based software, to model it as a single solid hollow conductor with the resistivity increased [7], [10]. This representation has been shown to be insufficient for accurate HV XLPE cable modelling [7], [8].

D. Outer insulation

The purpose of the cable outer coverings is mechanical protection against the surroundings. For XLPE cables, the outer insulation is made of high density polyethylene (the relative permittivity is approximately 2.3).

III. Modeling the Cable Sheath

As shown previously, the normal practice when modeling the sheath in EMT-based software is to represent it as a single solid conductor with a specific resistance, even though it physically consists of two conducting layers with a SC tape in between.

By use of high frequency field measurements, it has been shown how this representation of the sheath is inaccurate and gives errors in simulations for cables with cross bonding points, [8]. The topic of this paper is therefore to demonstrate an analysis of the real physical layout of the cable sheath and how to model it with a better accuracy in the software.

For analyzing the series impedance matrix of the cable, the internal loops of each cable are considered, see Fig. 2. The first loop is formed by the core conductor with the sheath as return and the second loop is formed by the sheath with the ground as return [11].

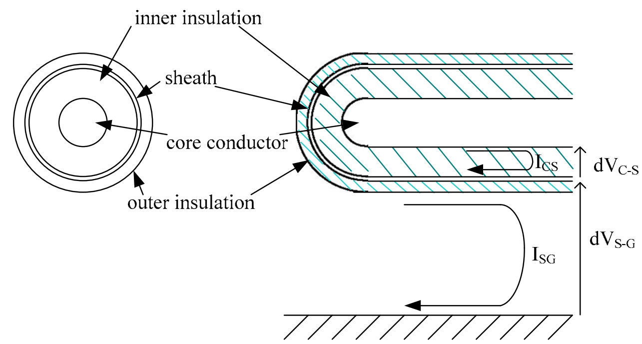

Fig. 2 Current loops in a single core coaxial cable. I_{CS} is the current in the loop formed by core conductor with sheath as return, I_{SG} is the current in the loop formed by sheath with ground as return, dV_{C-S} is the voltage difference between core conductor and sheath and dV_{S-G} is the voltage difference between the sheath and ground.

From Fig. 2 the impedance equivalent circuit for three single core cables can be derived, see Fig. 3, [12].

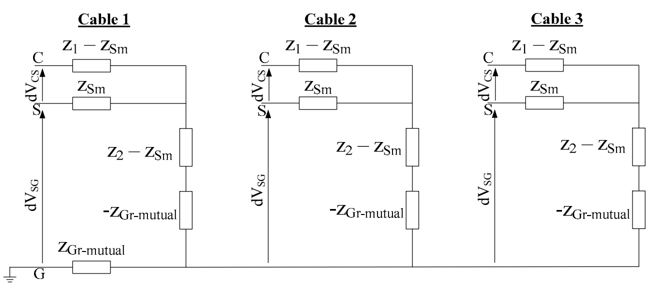

Fig. 3 Impedance equivalent circuit for the loop formation.

In this equivalent, the sheath is represented as a single conductor. The loop series impedance matrix is as shown in (1), where the superior indices *1*, *2* and *3* denote the respective cable number (phases).

$$\begin{bmatrix} Z_1^1 & -Z_{Sm}^1 & 0 & 0 & 0 & 0 \\ -Z_{Sm}^1 & Z_2^1 & 0 & Z_{Gr-mutual} & 0 & Z_{Gr-mutual} \\ 0 & 0 & Z_1^2 & -Z_{Sm}^2 & 0 & 0 \\ 0 & Z_{Gr-mutual} & -Z_{Sm}^2 & Z_2^2 & 0 & Z_{Gr-mutual} \\ 0 & 0 & 0 & 0 & Z_1^3 & -Z_{Sm}^3 \\ 0 & Z_{Gr-mutual} & 0 & Z_{Gr-mutual} & -Z_{Sm}^3 & Z_2^3 \end{bmatrix} \quad (1)$$

In order to correct for this sheath representation, the sheath mutual impedance, Z_{Sm}, needs to be split into three; impedance because of the wired sheath layer, because of the SC layer and because of the laminate layer. The impedances Z_1 and Z_2 are calculated by (2), [11], [13], [14], [15].

$$Z_1 = Z_{\text{C-outer}} + Z_{\text{CS-insul}} + Z_{\text{S-inner}} \quad (2a)$$

$$Z_2 = Z_{\text{S-outer}} + Z_{\text{SG-insul}} + Z_{\text{G}} \quad (2b)$$

Where $Z_{C\text{-}outer}$, $Z_{CS\text{-}insul}$, $Z_{S\text{-}inner}$, $Z_{S\text{-}outer}$, $Z_{SG\text{-}insul}$ and Z_G are the conductor series impedance, the inner insulation series impedance, the sheath inner series impedance, the sheath outer series impedance, the outer insulation series impedance and the earth self impedance respectively.

When calculating the sheath parts of (2), the impedances must be related to the correct layers of the split sheath. $Z_{S\text{-}inner}$ is therefore calculated by considering the wired sheath layer and $Z_{S\text{-}outer}$ is calculated by considering the laminate layer. This is based on the basic formulas for the sheath impedances given in [13] and shown in the appendix.

The two conducting layers are connected at each cable junction and cable end. An impedance equivalent including this layered sheath will therefore be a delta connection of impedances, see Fig. 4.

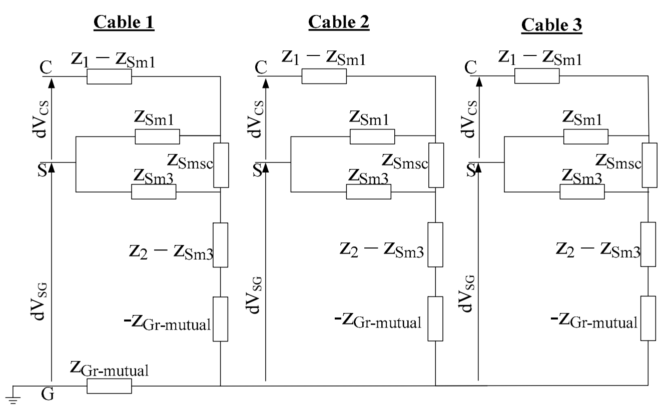

Fig. 4 Impedance equivalent circuit for the loop formation, where the layered sheath is included.

The split sheath mutual impedances are given by (3).

$$Z_{Smsc} = Z_3 - Z_{Sm1} - Z_{Sm3} \quad (3)$$

Where Z_{Sm1} and Z_{Sm3} are the mutual impedances of wired sheath layer (*Sm1*) and laminate sheath layer (*Sm3*) respectively and Z_3 is given by (4). Z_{Sm1} and Z_{Sm3} calculations are based on basic formulas given in [13] and shown in the appendix.

$$Z_3 = Z_{S1-outer} + Z_{SC-insul} + Z_{S3-innner} \quad (4)$$

Where $Z_{S1\text{-}outer}$, $Z_{SC\text{-}insul}$ and $Z_{S3\text{-}inner}$ are the *Sm1* layer outer series impedance, SC layer series impedance and the *Sm3* layer inner series impedance respectively calculated from the basic formulas given in appendix. Note that $Z_{SC\text{-}insul}$ can be neglected, as the thickness of the SC layer normally is less than 1 mm and therefore $\log(r_{ins-outer} / r_{ins-inner}) \approx 0$.

For representation of the cables impedance equivalent, this delta connection should be transformed to a star connection as shown in Fig. 5.

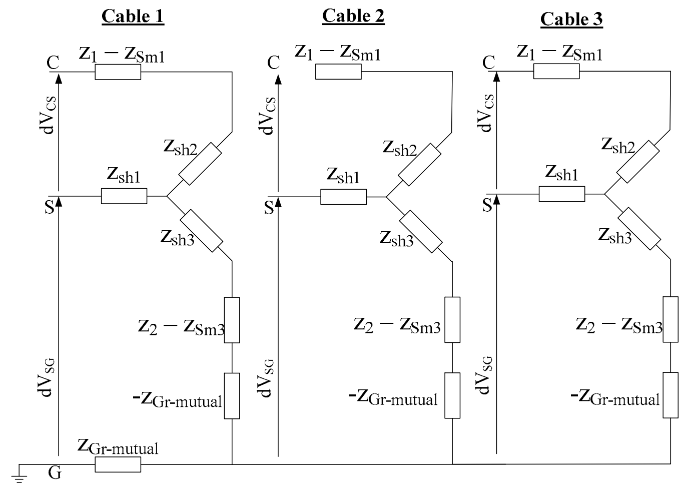

Fig. 5 Impedance equivalent circuit for the loop formation, where the layered sheath is included as a star connection.

The star connection impedances of Fig. 5 are calculated by the delta-star transformation and are given in (5).

$$Z_{sh1} = \frac{Z_{Sm1} \cdot Z_{Sm3}}{Z_{Smsc} + Z_{Sm1} + Z_{Sm3}} = \frac{Z_{Sm1} \cdot Z_{Sm3}}{Z_3} \quad (5a)$$

$$Z_{sh2} = \frac{Z_{Sm1} \cdot Z_{Smsc}}{Z_{Smsc} + Z_{Sm1} + Z_{Sm3}} = \frac{Z_{Sm1}(Z_3 - Z_{Sm1} - Z_{Sm3})}{Z_3} \quad (5b)$$

$$Z_{sh3} = \frac{Z_{Sm3} \cdot Z_{Smsc}}{Z_{Smsc} + Z_{Sm1} + Z_{Sm3}} = \frac{Z_{Sm3}(Z_3 - Z_{Sm1} - Z_{Sm3})}{Z_3} \quad (5c)$$

By this new modeling procedure for the sheath, the new loop series impedance matrix for the cable system in Fig. 5 can be calculated (6). This is done similarly to (1).

$$\begin{bmatrix} Z_{11}^1 & -Z_{sh1}^1 & 0 & 0 & 0 & 0 \\ -Z_{sh1}^1 & Z_{22}^1 & 0 & Z_{Gr-mutual} & 0 & Z_{Gr-mutual} \\ 0 & 0 & Z_{11}^2 & -Z_{sh1}^2 & 0 & 0 \\ 0 & Z_{Gr-mutual} & -Z_{sh1}^2 & Z_{22}^2 & 0 & Z_{Gr-mutual} \\ 0 & 0 & 0 & 0 & Z_{11}^3 & -Z_{sh1}^3 \\ 0 & Z_{Gr-mutual} & 0 & Z_{Gr-mutual} & -Z_{sh1}^3 & Z_{22}^3 \end{bmatrix} \quad (6a)$$

$$Z_{11} = Z_1 - Z_{Sm1} + Z_{sh2} + Z_{sh1} \quad (6b)$$

$$Z_{22} = Z_{sh1} + Z_{sh3} + Z_2 - Z_{Sm3} \quad (6c)$$

IV. Comparison of Field Measurements and Simulations

The new modeling procedure, by including the correct physical layout of the cable, is verified against field measurements on a 150 kV cable system in Denmark. The field test results are published as a part of the authors previous paper [8]. The principal of the field test setup is given in this paper.

A. Field measurements

In order to verify the new modeling procedur, the intersheath mode is excited. In other words, the current loop is formed by the sheath of one cable with the sheath of an adjacent cable as return. The reason for this is because analysis for long crossbonded cables has shown that when the intersheath mode is excited, the simulation results vary from measurements [7].

The cable line used in this paper consists of three phase cable systems with 150 kV single core 1200 mm^2 XLPE cables. The cables are laid in a tight trefoil with the bottom cables at 1.3 m depth, see Fig. 6, and the measurement setup is shown in Fig. 7.

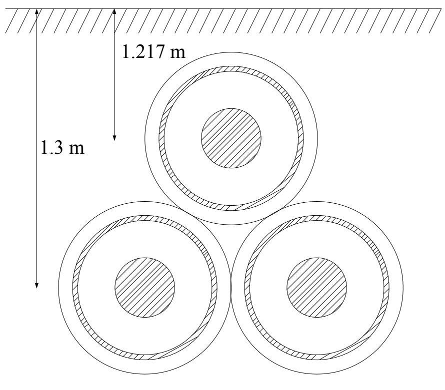

Fig. 6 Cross sectional layout for the cable system used in this paper.

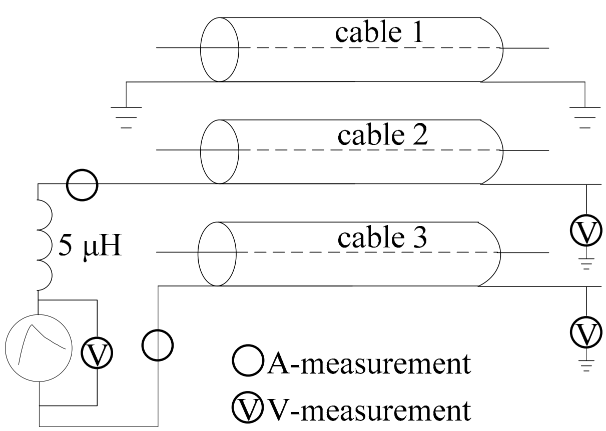

Fig. 7 Measurement setup for excitation of an intersheath mode.

In the measurement setup, a fast front impulse is used to energise between two sheaths (cable 2 and 3), while the third sheath is grounded. All core conductors are kept open at both sending and receiving end. Sheath voltages at both sending and receiving end of cables 2 and 3 and sheath currents of cables 2 and 3 at sending end were measured. The generator used is a HAEFELY PC6-288.1 surge tester. It is used to generate a 2 kV 1.2/50 µs impulse, see Fig. 8.

The generated fast front impulse is shown in Fig. 9.

Fig. 8 A HAEFELLY PC6-288.1 surge tester used to generate a 2 kV 1.2/50 µs impulse.

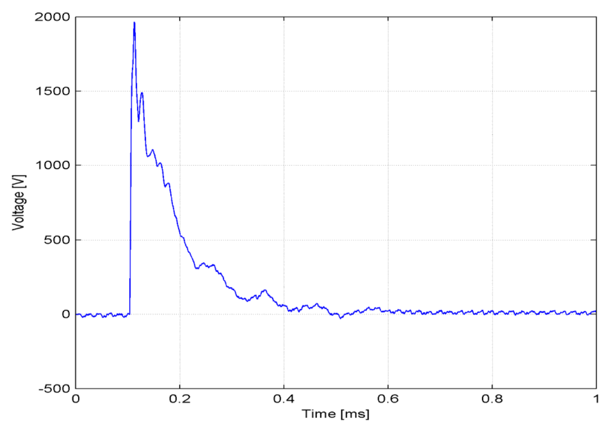

Fig. 9 Impulse voltage for excitation of the intersheath mode. This is the measured core voltage at the sending end of the excited sheath.

Identical Tektronix TDS 3014B oscilloscopes were used for measuring at both cable ends and the data was logged into a computer.

For all tests, Tektronix HV probes are used and for current measurements a PEM RGF15 was used to measure the sheath currents at the sending end.

B. Simulations and model verification

The cable parameters, used for modeling purposes, are given in Table I and a cross section of the cable is shown in Fig. 10. The parameters are already corrected according to the theory [7], [9].

The simulations are performed using the frequency dependent phase model in EMTDC/PSCAD [4] where the measured excitation voltage in Fig. 9 is used as an input to the simulation model. This ensures the excitation sending end voltage be identical for simulations and field tests.

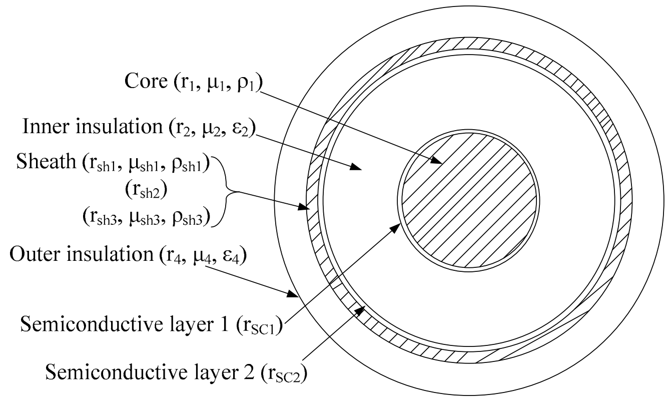

Fig. 10 Cross section of one single core cable showing the cable characteristic.

TABLE I
CABLE PARAMETERS

Parameter	**Value**
Stranded conductor, 1200mm^2 AL	r_1=20.75 mm, ρ_1=3.19·10^{-8} Ωm, μ_1=1.0
Semiconductive layer 1	r_{SC1}=22.25 mm
Inner insulation	r_2=39.25 mm, ε_2=2.68, μ_2=1.05
Semiconductive layer 2	r_{SC2}=40.25 mm
Stranded sheath, 95mm^2 Cu	r_{sh1}=41.96 mm ρ_{sh1}=0.91·10^{-7} Ωm, μ_{sh1}=1.0
Sheath SC	r_{sh2}=42.56 mm
Laminate sheath, Al	r_{sh3}=42.76 mm ρ_{sh3}=2.83·10^{-8} Ωm, μ_{sh3}=1.0
Outer insulation	r_4=47.94 mm, ε_4=2.3, μ_4=1.0
Cable length	l=1.78 km
Earth return	ρ_{earth}=100 Ωm

The comparison of field measurements and simulation results, for both modeling the sheath as a single conductor and for the new improved method of including the layered sheath are given in Fig. 11 and Fig. 12.

As can be seen in Fig. 11 and Fig. 12, then the simulating error lies in the amplitude and damping of the signals. Both simulation results have inadequate damping of higher frequency oscillations. This is because of wrong imaginary part of the series impedance in the simulation which can be explained by the lack of including the proximity effect in the simulation software. This has been shown by the authors of [7], [8], [16].

Fig. 11 and Fig. 12 also clearly show how the new and more correct method of modeling the layered sheath results in much smaller deviation between simulation results and field measurement. The reason for the better damping of simulations when modeling the layer more precisely using the new method described in this paper is a larger and more accurate impedance matrix, compared to the method of simplifying the sheath to only a single coaxial conducting layer.

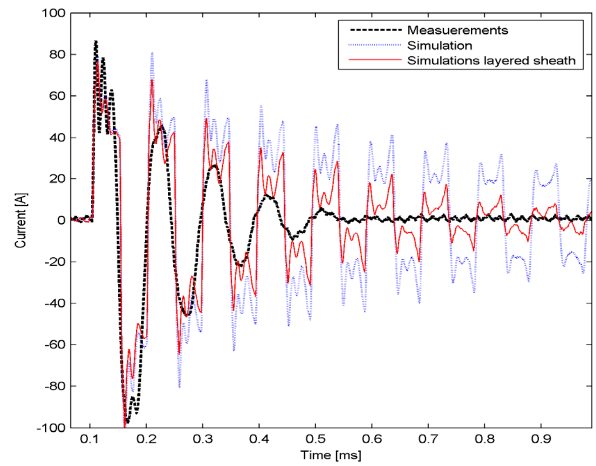

Fig. 11 Comparison of the sending end current on sheath of cable 2.

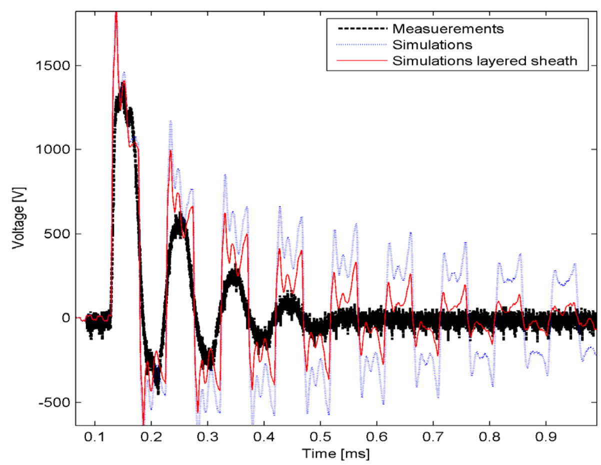

Fig. 12 Comparison of the receiving end voltage on sheath of cable 2.

V. SUMMARY AND CONCLUSIONS

This paper describes the special properties of an XLPE cable and addresses how the physical layout of the HV underground XLPE cable can be modelled in order to obtain more precise simulation result. Furthermore the improved modelling procedure is verified against field measurements, where the intersheath mode is explicitly excited. This is done as the presence of crossbonding points in long cables causes excitation of intersheath waves. The explicit excitation of the intersheath mode therefore verifies the model for the affect of crossbonding points in long HV AC cables, without having to take into account other modes of propagation as well.

The modelling procedure of simplifying the sheath to be represented as a single conducting coaxial layer is compared to the new method of modelling the more correct physical layout of the XLPE cable and dividing the sheath into layers. Both simulation results are compared to field measurements.

The simulations of the new modelling procedure and field test results agree quite well regarding the damping in the waveforms of the lower frequency components. This indicates that the cable model has been significantly improved. Both simulation results have though inadequate damping of high frequency transient oscillations. As the intersheath current propagates between the screens of adjacent cables, their propagation characteristics are also affected by proximity effects which are not taken into account by the simulation software when calculating the series impedance. Therefore, the remaining error of inadequate damping of oscillations appears in the simulations.

VI. Further work

The conclusions indicate that when modeling long cables with cross bonding points the correct physical layout of the sheath is important for correct simulation results. The paper gives a promising new method for modeling the sheath as a number of layers. Although the new modeling method results in less deviation between simulated and measured waveforms, the damping of high frequency oscillations is still inadequate. This is believed to be caused by proximity effect, which is not included in the simulation software. This effect therefore needs attention to further improve the simulation results for high frequency cable system studies.

VII. Appendix

The basic formulas for the individual series impedances of the cable are based on [11], [13] and [15].

The conductor series impedance:

$$Z_{\text{C-outer}} = \frac{\rho_C m_C}{2\pi r_C} \cdot \frac{I_0(m_C r_C)}{I_1(m_C r_C)} \qquad \text{(A1)}$$

Where the index C denotes the core conductor, ρ, m, r, I_0 and I_1 are the conductor resistivity, the reciprocal of the complex penetration depth, the conductor radius, the modified Bessel function of first kind of order 0 and of order 1 respectively.

The insulation series impedance:

$$Z_{\text{ins}} = \frac{j\omega\mu}{2\pi} \cdot \ln\left(\frac{r_{ins-outer}}{r_{ins-inner}}\right) \qquad \text{(A2)}$$

Where μ, $r_{ins-outer}$ and $r_{ins-inner}$ are the insulation permeability, the insulation outer and inner radius respectively.

The sheath inner and outer series impedance:

$$Z_{sh-inner} = \frac{\rho_{sh} m_{sh}}{2\pi r_{sh-i}} \coth(m_{sh}\Delta_{sh}) - \frac{\rho_{sh}}{2\pi r_{sh-i}(r_{sh-i} + r_{sh-o})} \qquad \text{(A3)}$$

$$Z_{sh-outer} = \frac{\rho_{sh} m_{sh}}{2\pi r_{sh-o}} \coth(m_{sh}\Delta_{sh}) - \frac{\rho_{sh}}{2\pi r_{sh-o}(r_{sh-i} + r_{sh-o})} \qquad \text{(A4)}$$

Where the index sh denotes the sheath, Δ, r_{sh-i} and r_{sh-o} are the thickness of the sheath, the sheath inner radius and the sheath outer radius respectively.

The sheath mutual impedance:

$$Z_{sh-m} = \frac{\rho_{sh} m_{sh}}{\pi(r_{sh-i} + r_{sh-o})} \operatorname{cosech}(m_{sh}\Delta_{sh}) \qquad \text{(A5)}$$

The ideal ground mutual impedances derived from Pollaczeck [17]:

$$Z_{Gr-mutual} = \frac{\rho m^2}{2\pi} \left[K_0(md) - K_0(mD) + \int_{-\infty}^{\infty} \frac{e^{-(d_i+d_j)\sqrt{\alpha^2+m^2}}}{|\alpha| + \sqrt{\alpha^2+m^2}} e^{j\alpha x} d\alpha \right] \qquad \text{(A6)}$$

Where K_0 is the modified Bessel function of second kind of order 0, d_i and d_j are the depth of cable i, j respectively and $d = \sqrt{x^2 + (d_i - d_j)^2}$, $D = \sqrt{x^2 + (d_i + d_j)^2}$ with x as the horizontal distance between cables i and j.

The earth self impedance is calculated from (A6) by exchanging x with r_{outer}, the cable outer radius and setting $d_i = d_j$, the cable depth.

VIII. Acknowledgment

The authors gratefully acknowledge the contributions of the Manitoba HVDC Research Centre for their support for the simulation studies presented in this document.

IX. References

[1] A. Ametani, "Wave propagation characteristics of cables," *IEEE Transactions on Power Apparatus and Systems*, vol. PAS-99, no. 2, pp 499-505, March/April 1980.

[2] L. Martí, "Simulation of transients in underground cables with frequency-dependent modal transformation matrices," *IEEE Transactions on Power Delivery*, vol. 3, no. 3, pp 1099-1110, July 1988.

[3] N. Nagaoka and A. Ametani, "Transient calculations on crossbonded cables", *IEEE Transactions on Power Apparatus and Systems*, vol. PAS-102, no. 4, pp 779-787, April 1983.

[4] A. Morched, B. Gustavsen, and M. Tartibi, "A universal model for accurate calculation of electromagnetic transients on overhead lines and underground cables," *IEEE Transactions on Power Delivery*, vol. 14, no. 3, pp. 1032-1038, July 1999.

[5] T.C. Yu and J.R. Martí, "zCable model for frequency dependent modelling of cable transmission systems," *IPST01 in Rio De Janeiro, Brazil*, paper no. IPST01-146, June 2001

[6] N. Nagaoka, T. Noda and A. Ametani, "Phase domain modelling of frequency-dependent transmission lines by means of an ARMA model", IEEE *Transactions on Power Delivery*, vol. 11, no. 1, pp. 401-411, January 1996.

[7] U.S. Gudmundsdottir, B. Gustavsen, C.L. Bak, W. Wiechowski and F.F. da Silva, "Field test and simulation of a 400 kV crossbonded cable system," *IEEE Transactions on Power Delivery*, unpublished, manuscript submitted in October 2009

[8] U.S. Gudmundsdottir, C.L. Bak, W. Wiechowski and F.F. da Silva, " Wave propagation and benchmark measurements for cable model validation," *IEEE Transactions on Power Delivery*, unpublished, manuscript submitted in November 2009

[9] J.A. Martinez, B. Gustavsen and D. Durbak, "Parameter determination for modelling system transients - part II: insulated cables," *IEEE Transactions of Power Delivery*, vol. 20, no. 3, pp. 1045-2050, July 2005.

[10] Gustavsen, B., 1993. A study of overvoltages in high voltage cables with emphasis on sheath overvoltages. Trondheim: NTH, Norges Tekniske Høgskole. ISBN: 82-7119-538-7.

[11] Dommel, H. W., 1996. EMTP Theory Book. 2nd ed. Vancouver: Microtran Power System Analysis Corporation.

[12] H. M. J. De Silva, "A robust multi-conductor transmission line model to simulate EM transients in underground cables," *IPST09 in Kyoto, Japan*, paper no. IPST09-175, June 2009

[13] L. M. Wedepohl, D. J. Wilcox, "Transient analysis of underground power-transmission systems," IEE Proceedings, vol. 120, no. 2, pp. 253-260, February 1973.

[14] G. Gaba, O. Saad and M. Giroux, "A closed-form approximation for ground return impedance of underground cables," IEEE Transactions on Power Delivery, vol. 11, no. 3, pp. 1536-1545, July 1996.

[15] A. Ametani, "A general formulation of impedance and admittance of cables," IEEE Transactions on Power Apparatus and Systems, vol. PAS-99, no. 3, pp. 902-910, May/June 1980.

[16] B. Gustavsen, J. Sletbak, and T. Henriksen, "Simulation of transient sheath overvoltages in the presence of proximity effects", *IEEE Trans. Power Delivery*, vol. 10, no. 2, pp. 1066-1075, April 1995

[17] V. F. Pollaczek, "Über die Felter der Wechselstromleitung mit Erde und der Horizontalantenne (in German) ", Elektrische Nachrichtentechnik, vol. 7, no. 4, pp. 295-304, May 1927.

X. Biographies

Unnur Stella Gudmundsdottir was born in Reykjavik in Iceland, on February 15, 1980. She received her B.Sc. degree in Electrical and Computer engineering in 2003 from The University of Iceland. She studied for the M.Sc. in Electric Power Systems at the institute of Energy Technology, Aalborg University in Denmark and received her degree in 2007 with speciality in state estimation and observability analysis. She received an honors price for her M.Sc. final thesis. She was a guest researcher at SINTEF in Norway in November 2008 and at Manitoba HVDC Research Centre in Canada during June-October 2009. Currently she is studying PhD at the Institute of Energy Technology, Aalborg University, in cooperation with the Danish Transmission system operator (Energinet.dk), where she also supervises students pursuing their M.Sc. degree in energy technology. Her PhD studies are focused on modelling of underground cable system at the transmission level.

H.M.J. De Silva was born in Ambalangoda, Sri Lanka. He received the B.Sc (eng) degree from university of Moratuwa, Sri Lanka in 2001 and PhD from University of Manitoba, Canada in 2009. His research interests are time domain modeling of multi-conductor underground cables and passivity enforcement of transmission lines. He is currently working at MHVDC Research Centre.

Claus Leth Bak was born in Århus in Denmark, on April 13, 1965. He graduated from High School in Århus and studied at the Engineering College in Århus, where he received the B.Sc. with honors in Electrical Power Engineering in 1992. He pursued the M.Sc. in Electrical Power Engineering with specialization in High Voltage Engineering at the Institute of Energy Technology (IET) at Aalborg University (AAU), which he received in 1994. After his studies he worked with Electric power transmission and substations with specializations within the area of power system protection at the NV Net transmission company. In 1999 he got employed as an assistant professor at IET-AAU, where he is holding an associate professor position today. His main research areas include corona phenomena on overhead lines, power system transient simulations and power system protection. He is the author/coauthor of app. 30 publications and IEEE Senior Member.

Wojciech Wiechowski (SMIEEE) received the M.Sc. degree from Warsaw University of Technology in 2001 and the Ph.D. degree from Aalborg University, Denmark in 2006. From 2001 to 2002 he worked for HVDC SwePol Link as a Technical Executor. In the period from 2002 to 2006 he was with the Institute of Energy Technology, Aalborg University, first as a PhD Student and later as an Assistant Professor. Since 2006 he has been employed in the Planning Department of the Danish TSO Energinet.dk where currently is a Senior Engineer. His recent activities are related to initiation and management of the cable technology development efforts of Energinet.dk in Denmark (all system technical performance issues as well as a variety of aspects related to cable lines as components) and initiation and convening of the Cigré WG C4.502 "Power system technical performance issues related to the application of long HVAC cables".